A&A 376, 793–802 (2001)
DOI: 10.1051/0004-6361:20011018

Astronomy & Astrophysics

High K–band surface brightness fluctuations in NGC 1427 and NGC 720*

S. Mei[1,2], M. Kissler–Patig[2], D. R. Silva[2], and P. J. Quinn[2]

[1] Observatoire Midi–Pyrénées, 14 Av. E. Belin, 31400 Toulouse, France
[2] European Southern Observatory, Karl-Schwarzschild-Strasse 2, 85748 Garching, Germany

Received 31 October 2000 / Accepted 6 July 2001

Abstract. We have observed K–band Surface Brightness Fluctuations (SBF) in NGC 1427 and NGC 720. We combine our measurements with distance measurements based on I–band SBF distance moduli and distance moduli derived by other distance indicators. When using distances from I–band SBF, we obtain $\overline{M}_K = -6.55 \pm 0.27$ for NGC 1427 and $\overline{M}_K = -6.43 \pm 0.18$ for NGC 720. When using an average of direct distance measurements, we obtain $\overline{M}_K = -6.17 \pm 0.23$ for NGC 1427 and $\overline{M}_K = -6.14 \pm 0.24$ for NGC 720. For both galaxies, $\overline{M}_K$ lies well above the average value used as a calibration for distance indication ($\overline{M}_K = -5.61 \pm 0.12$ Jensen et al. 1998). In NGC 720 the high K–band SBF are most probably due to an intermediate-age population. However, there is no hint from current data for any anomaly in the stellar population of NGC 1427. These large variations of $\overline{M}_K$ in several galaxies underline once more the need for a better understanding of $\overline{M}_K$ as a function of stellar population properties (Mei et al. 2001b; Liu et al. 2001), especially with respect to the potential presence of intermediate–age populations.

Key words. galaxies: distances – individual: NGC 1427, NGC 720

1. Introduction

Surface Brightness Fluctuations (SBF) observed in the diffuse light of galaxies were found not only to be a good secondary distance indicator (e.g. Tonry & Schneider 1988; Tonry et al. 2000), but also to probe the underlying stellar populations (Jensen et al. 1998; Liu et al. 2000; Blakeslee et al. 2001; Mei et al. 2001b). By definition, the SBF is sensitive to the brightest stellar populations in the galaxy. In early-type galaxies, the red giants contribute the most to the SBF amplitude. This motivates an application of the method in the near-infrared, where the light of these stars dominates even more over the rest of the stellar population.

The SBF method for distance measurement is based on the Poissonian statistics of unresolved stars in galaxy images. The Poissonian distribution of the stars in each pixel produces fluctuations whose variance is proportional to the square of the galaxy distance. The SBF amplitude is defined as the second moment of the stellar population flux normalized to the mean flux (Tonry & Schneider 1988). The method is mainly applied to elliptical galaxies and bulges of spirals, where dust patches do not alter the measurement of the fluctuations.

I–band Surface Brightness Fluctuations have been successfully used to measure galaxy distances from the ground up to 4000 $\mathrm{km\,s^{-1}}$ and with the Hubble Space Telescope up to 7000 $\mathrm{km\,s^{-1}}$ (Sodemann & Thomsen 1995; Sodemann & Thomsen 1996; Ajhar et al. 1997; Tonry et al. 1997; Thomsen et al. 1997; Lauer et al. 1998; Pahre et al. 1999; Blakeslee et al. 1999a; Tonry et al. 2000; Mei et al. 2000; Tonry et al. 2001). The absolute scale of this distance indicator has been calibrated on a sample of ellipticals and spiral bulges with Cepheid distance measurements. These galaxies show a linear relation between I–band absolute amplitude and galaxy color $V-I$ (Tonry et al. 2000; Ferrarese et al. 2000a), which implies the need for a color correction to the uncorrected I–band SBF measurements in order to be used as an accurate distance indicator.

Recently SBF measurements were extended to the near-infrared: in the K–band from the ground (Luppino & Tonry 1993; Pahre & Mould 1994; Jensen et al. 1996; Jensen et al. 1998; Jensen et al. 1999; Mei et al. 2001b), and in the F160W filter on HST (Jensen et al. 2001). At present K–band Surface Brightness Fluctuations have been measured from the ground for a sample of about twenty galaxies up to 7000 $\mathrm{km\,s^{-1}}$ (Pahre & Mould 1994; Jensen et al. 1998; Jensen et al. 1999; Jensen et al. 2001;

Send offprint requests to: S. Mei,
e-mail: `mei@ast.obs-mip.fr`

* Based on observations performed at the European Southern Observatory, La Silla, Chile; ESO program No. 62.N-0568.

Mei et al. 2001b). Near-infrared measurements are interesting for various reasons. First, red giants have predicted SBF amplitudes about thirty times higher in the K–band than in the I–band. Second, in the K–band the color contrast between SBF and fluctuations from external sources (globular clusters and background galaxies) is higher. Third, the seeing is usually better in the infrared than in optical bands, which enhances the SBF contrast. Finally, for the purpose of distance measurements, initial K–band observations suggested that the absolute SBF magnitude M_K varied very little from galaxy-to-galaxy for ellipticals with $V-I$ colors between 1.15 and 1.25 mag (Pahre & Mould 1994; Jensen et al. 1996; Jensen et al. 1998). This would imply that, in this galaxy color range, K–band observations do not need to be calibrated for differences in the stellar populations among galaxies, as it is required in the I–band. And, at present, most of the observations (Pahre & Mould 1994; Jensen et al. 1998; Jensen et al. 1999) show absolute K–band SBF for ellipticals with $V-I$ colors between 1.15 and 1.25 mag, that are consistent with old, near–solar metallicity stellar populations.

The above reasons would suggest that K–band SBF can extend distance measurements farther than were possible in the I–band. However, an evaluation of the error budget in I and K (Mei et al. 2001a) shows that, for correct estimation of the external source contribution to the measurements, the high sky background in the K–band from the ground is still a limiting factor, and that it counter-balances the advantages of the K–band. A breakthrough in distance measurements is therefore only expected once high-resolution space-based near-IR imagers become regularly available (e.g. a refurbished NICMOS or the future Next Generation Space Telescope).

Stellar population studies based on SBF, however, can already profit from K–band data. Theoretical predictions (Jensen et al. 1998; Mei et al. 1999; Liu et al. 2000; Mei et al. 2001a; Blakeslee et al. 2001) on K–band SBF absolute amplitudes are contradictory. Recent models based on Bruzual & Charlot (2000) stellar population models (Liu et al. 2000; Mei et al. 2001a) predict K–band SBF amplitudes to become brighter for redder populations, while independent models by Blakeslee et al. (2001) predict K–band SBF absolute amplitudes to become fainter for redder populations. Moreover, galaxies with anomalous high K–band fluctuations were observed (Pahre & Mould 1994; Jensen et al. 1996; Jensen et al. 1998; Mei et al. 2001a). These could either be due to the presence of an anomalous stellar population, or by a (still to be explained) departure from the color – SBF magnitude relation for blue galaxies (Mei et al. 2001b; Liu et al. 2001). Indeed, the relation between absolute SBF magnitude and galaxy color was empirically established only for galaxies with $(V-I) > 1.15$ (Jensen et al. 1998). Clearly, the K–band sample has to be extended to improve our understanding of the stellar population effects, on the one hand to gain insight into the stellar content of early-type galaxies, and on the other hand to allow accurate distance measurements with this method.

In the following, we present high signal-to-noise K–band SBF in two early-type galaxies within $\sim$1500 km s^{-1}, NGC 1427 and NGC 720. NGC 1427 was expected to be a standard intermediate luminosity galaxy in the Fornax cluster, that we expected to contrast with the isolated, X-ray bright galaxy NGC 720, which was reported to host a young population, mainly based on Balmer line indices (Trager et al. 2000). General properties of these galaxies are summarized in Table 1. We combine our measurements with known distances to derive absolute SBF amplitudes $\overline{M}_K$, and investigate a possible dependence on stellar populations. We further compare the derived $\overline{M}_K$ with the Jensen et al. (1998) sample. In Sect. 2 we describe our observations, and in Sect. 3 the SBF analysis. The results and a summary of this analysis are presented in Sects. 4 and 5.

2. Observations

The two galaxies were observed at the 3.5 m New Technology Telescope (NTT) at the European Southern Observatory at La Silla, Chile, on 4 December 1998. The images were obtained with SOFI (Son OF ISAAC, a near-infrared imaging spectrometer) equipped with an Hawaii HgCdTe 1024×1024 detector array. The gain is 5.5 e$^-$/ADU, the read out noise 2.1 ADU, the dark current <0.1 e$^-$/s. We used the Large Field imaging mode, with a pixel scale equal to $0.29''$/pixel and a field of view $4.9' \times 4.9'$.

The aim of the run was the study of the globular cluster populations of these galaxies in the near infrared. These results will be presented in separate papers. The deep exposures were also well suited for SBF analysis. We have reduced the data in a different way than the analysis for globular cluster studies, being careful not to alter the photon statistics on the individual pixels. The images were obtained in the K short filter (K_s), centered at 2.16 μm. The K_s filter is centered at shorter wavelength than the standard K filter to reduce thermal background and at larger wavelength than the K' filter (Wainscoat & Cowie 1992). Pahre & Mould (1994) estimated the difference between this filter and the standard K–band to be of the order of 0.02 magnitudes for elliptical galaxies. Given the lack of proper conversion, we do not translate our results to the standard K–band filter. Thus, we accept a negligible potential systematic error of the order of 0.02 (smaller than the error in our calibration) in our SBF magnitudes when compared to results obtained in other K–band filters, and warn that our SBF magnitudes are measured in the K_s filter.

The seeing, as measured from the FWHM of our stellar objects, was $0.75''$ for NGC 720 and $0.77''$ for NGC 1427. The data were calibrated using faint standard stars from Hunt et al. (1998, UKIRT faint standard system) observed throughout the night. The zero-point and extinction coefficient were found to be 22.34 ± 0.04 and 0.05 ± 0.02, respectively. The sky brightness was on average 12.76 mag arcsec^{-2}. The observing procedure consisted of

Table 1. General properties of NGC 1427 and NGC 720, taken from Tully (1988), Poulain (1988), Poulain & Nieto (1994), de Vaucouleurs et al. (1991), Tonry et al. (2001).

Name	RA	DEC	l	b	Type	m_V	$(V-I)$	V_0
	(2000)	(2000)	deg	deg		mag	mag	$\mathrm{km\,s^{-1}}$
NGC 1427	03 42 19	−35 23 36	236.60	−52.85	E3	11.04	1.152	1416
NGC 720	01 53 00	−13 44 00	173.03	−70.35	E5	10.17	1.214	1716

taking alternate dithered background-galaxy-background sets for a total exposure time on the galaxies equal to 6400 s for NGC 720 and 4000 s for NGC 1427. We subtracted close background images from the galaxy images and divided the resulting images by a normalized dome flat field (the dark current was subtracted by this operation). Bad pixels and cosmic rays were eliminated by a sigma clipping algorithm while combining the images using the IRAF[1] task IMCOMBINE. Sub-pixel registration was not used to avoid introducing correlated noise between the pixels in the images.

3. Surface brightness fluctuations analysis

3.1. Measure of SBF magnitudes

The data were analyzed by the SBF extraction standard technique used by Tonry & Schneider (1988). The first step is to subtract a smooth galaxy model from the combined, background-subtracted image. We build such a model by fitting the galaxy isophotes. To do so, bright external sources are masked in the fitting. Additional, fainter, external point sources (globular clusters and background galaxies) are identified, fitted and subtracted using Sextractor (Bertin & Arnouts 1996). The residual image is then smoothed with a median filter on a scale ten times the width of the PSF and subtracted from the original image. This accounts for residual background-subtraction errors. The fitting of the galaxy isophotes is then iterated to obtained the final galaxy model.

The original image gets divided by the square root of our galaxy model in order to obtain constant SBF amplitudes across the image. Finally, the image power spectrum is calculated on different annuli. In each annulus we calculated a completeness function adding simulated point source images to the original, galaxy subtracted image. The external point sources were masked up to a cut-off magnitude $m_{\rm cut}$. We give the value of $m_{\rm cut}$ for each annulus in Tables 2 and 3. The external source luminosity functions for NGC 1427 and NGC 720 are shown respectively in Figs. 1 and 2.

A point spread function (PSF) profile was determined from the bright stars in the image and normalized it at 1 $\mathrm{ADUs^{-1}}$. From this profile, the power spectrum of the PSF was calculated. In each annulus the image power spectrum was calculated, normalized to the number of non-zero points and azimuthally averaged. The power spectrum consists of two components: the constant power spectrum due to the white noise, P_1, and the power spectrum of the fluctuation (including unresolved point sources), P_0, convolved in the spatial domain with the known PSF. In the Fourier domain this last term is given by a constant P_0 multiplied by the power spectrum of the PSF:

$$E_{\rm gal} = P_0\ E_{\rm PSF} + P_1. \tag{1}$$

A robust linear least square fit was made, minimizing absolute deviation (Press et al. 1992), from which P_0 and P_1 were derived. We excluded low wave number points from the fit, since they are contaminated by the galaxy subtraction and subsequent smoothing, as well as residual background variance contribution. We have subtracted from P_0 the contribution of point source fluctuations $P_{\rm es}$, estimated from the equations:

$$P_{\rm es} = \sigma_{\rm gc}^2 + \sigma_{\rm bg}^2 \tag{2}$$

following, e.g. Blakeslee & Tonry (1995); $\sigma_{\rm gc}^2$ is the contribution to the fluctuations given by globular clusters, $\sigma_{\rm bg}^2$ is the contributions by background galaxies. We assumed for the luminosity function of the globular clusters:

$$N_{\rm gc}(m) = \frac{N_{\rm gc}^{\rm o}}{\sqrt{2\pi}\sigma}{\rm e}^{\frac{-(m-m_{\rm peak})^2}{2\sigma^2}}, \tag{3}$$

with $\sigma = 1.2$, $m_V^{\rm gc} = 23.78$ for NGC 1427 (Kohle et al. 1996), and $\sigma = 1.26$, $m_V^{\rm gc} = 24.10$ for NGC 720 (Kissler-Patig et al. 1996). To derive $m_K^{\rm gc}$ we assume a mean globular cluster color of $(V-K) = 3.0$ (as derived from our globular cluster studies in elliptical galaxies). For the background galaxies we assume a power-law luminosity function

$$N_{\rm bg}(m) = N_{\rm bg}^{\rm o} 10^{\gamma m} \tag{4}$$

with $\gamma = 0.3$ (Cowie et al. 1994). We have verified that exact details in the adopted globular cluster and background galaxy luminosity functions have little effect on the final measurement of SBF amplitudes, as pointed out e.g. from Blakeslee et al. (1999a). We estimated $N_{\rm gc}^{\rm o}$ and $N_{\rm bg}^{\rm o}$ per pixel, from the fitting of the composite luminosity function that we have from the external sources extracted from the image and calculated $P_{\rm s}$ as the sum of:

$$\sigma_{\rm gc}^2 = \tfrac{1}{2} N_{\rm gc}^{\rm o} 10^{0.8[m_1 - m_{\rm peak} + 0.4\sigma^2 \ln(10)]} \\ {\rm erfc}\left[\frac{m_{\rm cut} - m_{\rm peak} + 0.8\sigma^2 \ln(10)}{\sqrt{2}\sigma}\right] \tag{5}$$

[1] The Image Reduction and Analysis Facility (IRAF) is distributed by the National Optical Astronomy Observatories.

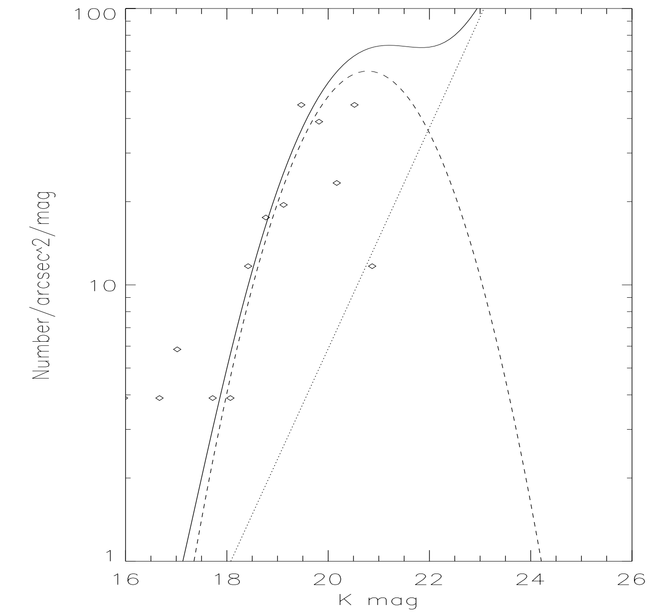

Fig. 1. We show for NGC 1427 the external source luminosity function. The diamonds are the number of sources per magnitude and per square arcminute, that we have detected in the total area where we have calculated SBF. Note that the last points are affected by incompletness. The continuous line shows the sum of the globular cluster and the background-galaxy luminosity functions. The dashed and dotted lines show separately the contributions of the globular cluster luminosity function and the background-galaxy luminosity function, respectively.

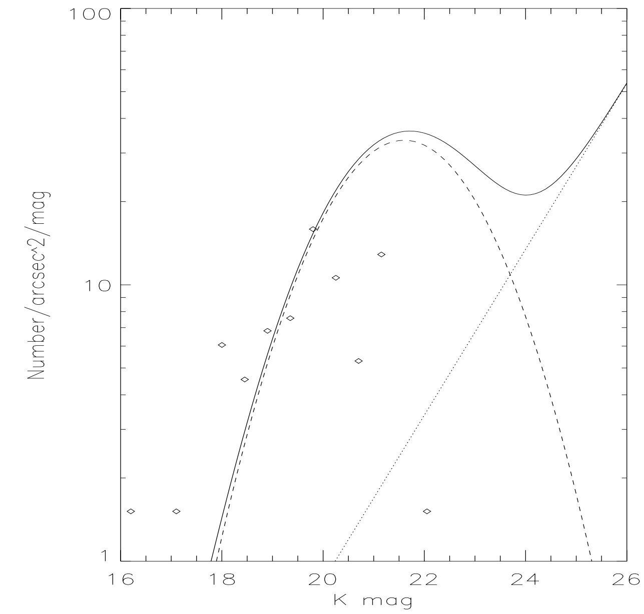

Fig. 2. Identical to Fig. 1 but for NGC 720.

and

$$\sigma_{\rm bg}^2 = \frac{N_{\rm bg}^{\circ}}{(0.8-\gamma)\ln(10)} 10^{0.8(m_1 - m_{\rm cut}) + \gamma(m_{\rm cut})}. \quad (6)$$

m_1 is the zero magnitude which corresponds to a flux of 1 ADU s^{-1}. We used the $m_{\rm cut}$ given in Tables 2 and 3. We calculated the SBF amplitude as:

$$\overline{m}_K = -2.5\log(P_0 - P_{\rm es}) + m_1 - \epsilon_{\rm ext}\sec(z) \quad (7)$$

where $\epsilon_{\rm ext}$ the extinction coefficient, $\sec(z)$ the airmass for the observations. Color term and redshift correction are negligible (Liu et al. 2000). We did not apply any galactic extinction correction, given the $E(B-V) = 0.011$ for NGC 1427 and $E(B-V) = 0.016$ for NGC 720 (Schlegel et al. 1998), and $A_K = 0.004$ for NGC 1427 and 0.006 for NGC 720.

We measured $\epsilon_{\rm ext} = 0.05 \pm 0.02$ and $m_1 = 22.34 \pm 0.04$ (see Sect. 2). The effective airmass was $\sec(z) = 1.3$ for NGC 1427, and $\sec(z) = 1.14$ for NGC 720. We have calculated the error on $\overline{m}_K$ as the standard deviation of the different annuli considered plus the entire field. To the fitting errors we add in quadrature the error due to the photometric calibration (zero point and extinction coefficient uncertainties) and to external source residual contribution subtraction.

3.2. NGC 1427

We have calculated the SBF amplitudes in successive circular regions from $9''$ to $33''$. We show our power spectrum fitting of NGC 1427 in Fig. 3. The results for each annulus are listed in Table 2. We give the errors on SBF magnitudes for each annulus as the standard deviations among different wavelength cuts.

We find a value of $\overline{m}_K = 25.31 \pm 0.08$. The error on m_K is calculated by adding in quadrature the standard deviation of the magnitudes derived in each annulus, divided by the number of considered values.

3.3. NGC 720

In this galaxy the central region was excluded from our analysis because of the difficulty in the galaxy profile subtraction. We have calculated SBF amplitudes in successive circular regions from $44''$ to $67''$. The power spectrum for NGC 720 is shown in Fig. 4. We show the results for each annulus in Table 3. We give the errors on SBF magnitudes for each annulus as the standard deviations among different wavelength cuts.

We derive a value of $\overline{m}_K = 25.78 \pm 0.07$. The error on m_K is calculated as for NGC 1427.

4. The distances to NGC 1427 and NGC 720

In order to derive absolute K–band SBF magnitudes, we need to know the distance to our target galaxies. The only direct distance measurements for these galaxies are based on the globular clusters luminosity function (GCLF) and I–band SBF. We discuss these in turn, attempt to bring the GCLF measurements onto a homogeneous scale, and present other distance measurements for the Fornax clusters to which NGC 1427 belongs.

Table 2. SBF measurements for various annuli of NGC 1427.

Annulus (arcsec)	P_0	σ_{P_0}	P_0/P_1	$P_{\rm es}$	$\overline{m}_K$	$\sigma_{\overline{m}_K}$	$m_{\rm cut}$
9–14	0.064	0.004	7	0.01	25.46	0.09	19.9
14–19	0.050	0.004	4	0.01	25.77	0.11	19.9
19–23	0.073	0.002	3	0.01	25.28	0.05	19.9
23–28	0.072	0.003	2	0.01	25.30	0.05	19.9
28–33	0.097	0.007	1	0.01	24.93	0.09	19.9
9–33	0.083	0.002	3	0.01	25.12	0.05	19.9
Mean	–	–	–	–	25.31	0.04	–

Table 3. SBF measurements for various annuli of NGC 720.

Annulus (arcsec)	P_0	σ_{P_0}	P_0/P_1	$P_{\rm es}$	$\overline{m}_K$	$\sigma_{\overline{m}_K}$	$m_{\rm cut}$
44–48	0.057	0.002	5	0.023	25.95	0.09	19.9
48–53	0.071	0.002	4	0.023	25.58	0.06	19.9
53–58	0.052	0.002	3	0.023	26.13	0.07	19.9
58–62	0.064	0.002	3	0.023	25.74	0.05	19.9
62–67	0.060	0.002	2.5	0.023	25.85	0.06	19.9
44–67	0.067	0.002	3	0.023	25.39	0.05	19.9
Mean	–	–	–	–	25.78	0.07	–

4.1. NGC 1427

An I–band SBF distance was derived for NGC 1427 by Tonry et al. (2001). They obtained a distance modulus of $(m-M) = 31.86 \pm 0.26$.

The distance to NGC 1427, as derived from the recession velocity of the galaxy (see Table 1, matching within 10 km s^{-1} the mean velocity of the Fornax cluster), an adopting a Hubble constant of $H_0 = 72 \pm 8$ km s^{-1} Mpc^{-1} (Freedman et al. 2001), is 19.7 ± 2.2 Mpc, or $(m-M) = 31.47 \pm 0.23$.

The other direct distance measurement was obtained by Kohle et al. (1996) using the GCLF. We revise their result to put it onto a homogenous scale, since the calibration of the method is applied heterogeneously in the literature (e.g. Kissler-Patig 2000). To do so, we use their observed GCLF turn-over magnitudes, correct these for stellar population effects (see Ashman et al. 1995) and calibrate the later using the absolute turn-over magnitudes given in Della Valle et al. (1998), and Drenkhahn & Richtler (1999). Note that the final distance will be independent of the LMC distance (see Della Valle et al. 1998), that is independent from the Cepheid distance and thus from the I–band SBF distance to the galaxy.

We use, from Kohle et al. (1996), the mean of their t-function and Gaussian fits (differing by 0.10 to 0.15) for the turn-over magnitudes in V and I ($v_0^{\rm TO} = 23.71 \pm 0.20$, $i_0^{\rm TO} = 22.27 \pm 0.14$). To these we apply the corrections for stellar population effects given by Kohle et al. ($\Delta V = 0.10$, $\Delta I = 0.05$), and apply the calibration given in Della Valle et al. (1998) and Drenkhahn & Richtler (1999) derived from the Milky Way system ($V_0^{\rm TO} = -7.62 \pm 0.06$, $I_0^{\rm TO} = -8.60 \pm 0.07$). The mean of the resulting distance moduli derived for V and I is $(m-M) = 31.02 \pm 0.25$.

The scatter among the derived distances is large, but within 2σ. The mean is close to the distance expected from recession velocity only, and to the mean distance of the Fornax cluster (see below). Thus the distance derived from I–band SBF seems slightly too high, while the distance derived from GCLF appears slightly too low.

In this paper, we do not include in the estimated errors on $\overline{M}_K$ the systematic error due to the Cepheid calibration of the I–band SBF, that amounts to 0.16 mag.

4.2. NGC 1427 as a member of the Fornax cluster

The Fornax cluster is at a distance comparable to the Virgo distance and has been well studied in terms of distance measurements by Surface Brightness Fluctuations in the I– and in the K–band (Jensen et al. 1998), by Planetary Nebulae Luminosity Functions (McMillan et al. 1993), by Cepheids (Madore et al. 1999), by Tully-Fisher, Fundamental Plane (de Vaucouleurs 1993), and Globular Cluster Luminosity Function (Kohle et al. 1996; Della Valle et al. 1998; Grillmair et al. 1999).

Most data can be found in the compilation of Ferrarese et al. (2000a,b), where the mean to the Fornax cluster is given with $(m-M) = 31.52 \pm 0.03$.

With respect to the Virgo cluster, Fornax has the advantage of not presenting a significant depth i.e. no high dispersion in distances to the individual galaxies (see for example Madore et al. 1999; Drinkwater et al. 2001). From

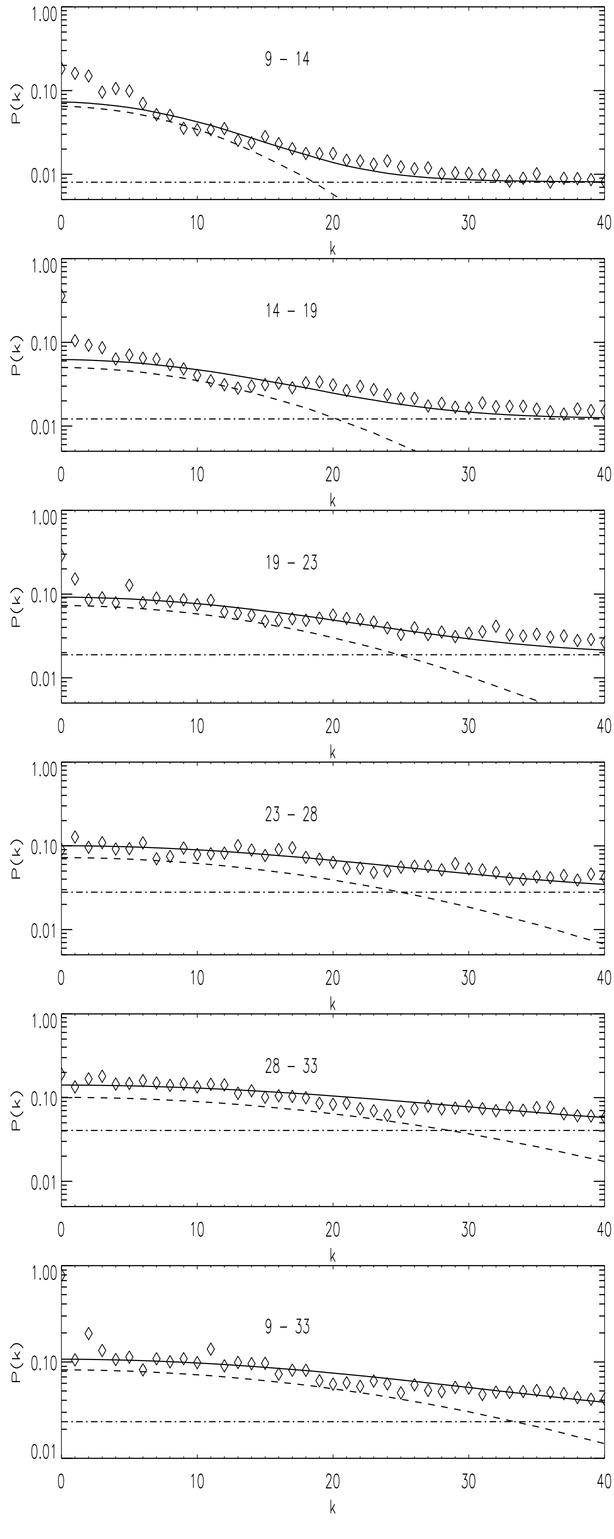

Fig. 3. We show the NGC 1427 power spectrum as fitted in five different annuli of width ≈5″ and on the full field up to ≈33″. The fit of the power spectrum is given by the continue line, the PSF power spectrum by the dashed line and the dashed-dotted line is the fitted constant white noise spectrum.

Drinkwater et al. (2001), NG 1427 is clearly associated with the core of the Fornax cluster, which justifies using distances to this cluster as approximate distances to NGC 1427.

A GCLF distance on the same scale as discussed in the last section was derived for NGC 1380 (also belonging to the cluster core) by Della Valle et al. (1998) who obtained $(m - M) = 31.35 \pm 0.16$.

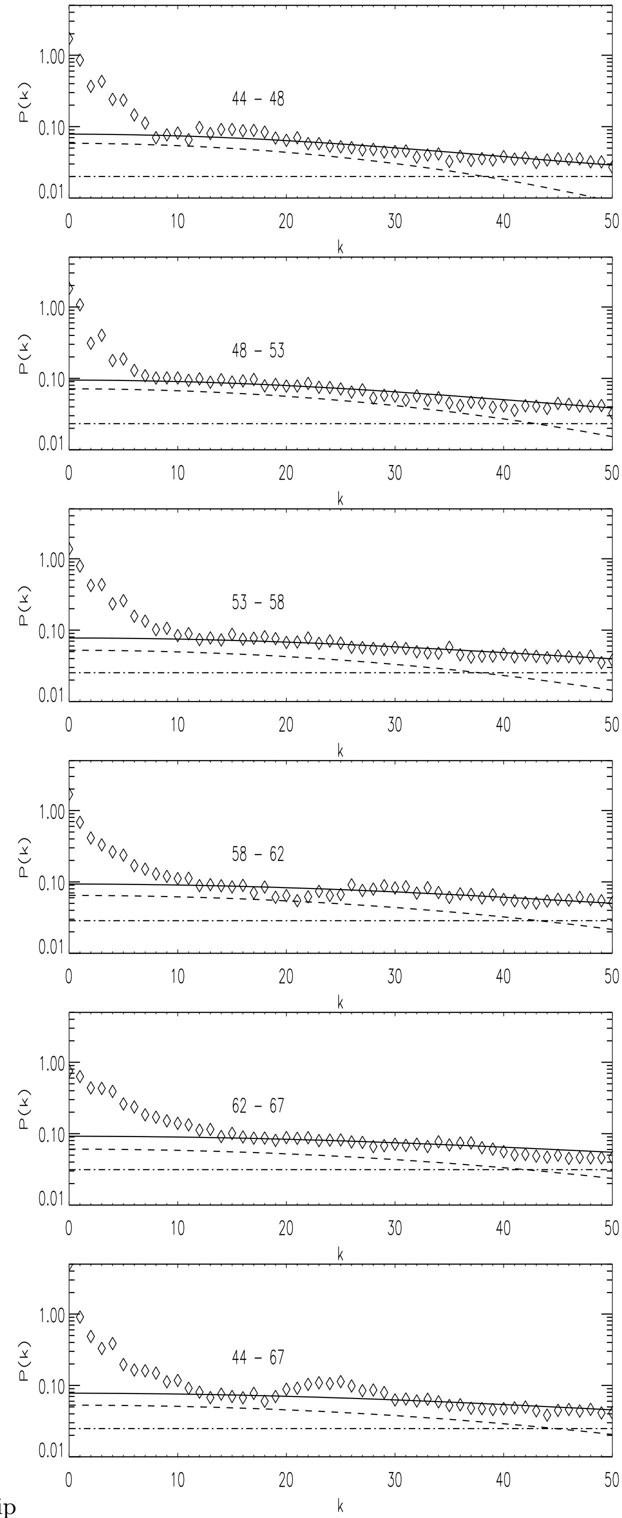

clip

Fig. 4. We show the NGC 720 power spectrum as fitted in five different annuli of width ≈5″ and on the full field up to ≈67″. The fit of the power spectrum is given by the continue line, the PSF power spectrum by the dashed line and the dashed-dotted line is the fitted constant white noise spectrum.

4.3. NGC 720

Tonry et al. (2000) also derived the I–band SBF distance to NGC 720. They obtained a distance modulus of $(m - M) = 32.21 \pm 0.17$.

The distance to NGC 720, as derived from the recession velocity of the galaxy (see Table 1), an adopting a Hubble constant of $H_0 = 72 \pm 8$ km s^{-1} Mpc^{-1}, is 23.8 ± 2.7 Mpc or $(m - M) = 31.89 \pm 0.22$.

GCLF turn-overs were measured in the V–band by Kissler-Patig et al. (1996, $v_0^{\rm TO} = 24.03 \pm 0.20$ as a mean of t-function and Gauss fit), and in the B– and I–band by Chapelon et al. (in preparation, $b_0^{\rm TO} = 25.2 \pm 0.4$, $i_0^{\rm TO} = 23.0 \pm 0.9$). The mean color of the globular cluster system is $(B-I) = 1.86$ (Chapelon et al. in preparation) compared to $(B-I) = 1.64$ for the Milky Way. The mean color was transformed into a mean metallicity of [Fe/H] $= -0.75$ dex using the relation given in Barmby et al. (2000). Corrections to the GCLF of $\Delta B = 0.27$, $\Delta V = 0.17$, and $\Delta I = 0.08$ were derived according to Ashman et al. (1995). The resulting distance moduli are $(m-M)_V = 31.48 \pm 0.21$, $(m-M)_B = 32.01 \pm 0.41$, $(m-M)_V = 31.52 \pm 0.90$, and their weighted mean is $(m-M) = 31.67 \pm 0.29$.

As for NGC 1427, the SBF and GCLF measurements only overlap in the 2σ range, the SBF measurement appearing high, the GCLF measurement being low.

All the distances are summarised in Table 4.

5. Absolute K–band SBF magnitudes

We derive the absolute K–band SBF magnitudes based on the various distances presented above, and put the measurements on a common scale with previous measurements. All our results are shown in Table 4.

5.1. NGC 1427

We first derive the K–band SBF magnitude for NGC 1427 using I–band SBF distances from Tonry et al. (2001), following the standard procedure for deriving $\overline{M}_K$ for calibration (Jensen et al. 1998; Liu et al. 2001). We obtain $\overline{M}_K = -6.55 \pm 0.27$. This amplitude is higher than the Jensen et al. (1998) calibration for the K–band absolute magnitude $\overline{M}_K = -5.61 \pm 0.12$, at the three sigma level.

The I–band SBF derived $\overline{M}_K$ strongly depends on the I–band SBF measurements. The I–band SBF distance modulus for this galaxy is around 0.5 mag fainter than the average Fornax distance modulus, while recession velocity studies (Drinkwater et al. 2001) indicates that this galaxy is clearly associated with the core of the Fornax cluster (see Sect. 4.2). We derive $\overline{M}_K = -6.18 \pm 0.09$ from the I–band SBF distance derived for the Fornax cluster, in good agreement with the values derived using other distance determinations (see below). Again, this amplitude is high with respect to the standard Jensen et al. (1998) calibration. However, the *apparent* $K_{\rm s}$ fluctuations that we derive are in good agreement with Liu et al. (2001) measurement. Thus, the discrepancy in $\overline{M}_K$ appears real unless we under-estimated the distance to NGC 1427 by 0.5 magnitudes, which appears extremely unlikely (see last section). Indeed, when all distance moduli are used and averaged, we obtain an average $\overline{M}_K = -6.14 \pm 0.27$ from the galaxy distance moduli and $\overline{M}_K = -6.20 \pm 0.18$ from Fornax distance moduli ($\overline{M}_K = -6.18 \pm 0.24$ when we use all values for galaxy and cluster). One could argue that, due to the high error on $\overline{M}_K$, and due to the uncertainty on the galaxy distance moduli, these last three results are consistent within the one sigma level with the new Liu et al. (2001) calibration of $\overline{M}_K$ versus $V-I$, valid for a wider range of galaxy colors ($(V-I)$ from 1.05 and 1.25), that predicts for this galaxy $\overline{M}_K = -5.85 \pm 0.08$. But note that Liu et al. also found NGC 1427 to exhibit large K–band SBF.

5.2. NGC 720

Combining our K–band SBF measurements and the I–band SBF distance derived by Tonry et al. (2001), we obtain $\overline{M}_K = -6.43 \pm 0.18$. When other distance moduli are used and averaged we obtain $\overline{M}_K = -6.14 \pm 0.24$. These high amplitudes are again inconsistent with the Jensen et al. (1998) average for standard red elliptical. From the Liu et al. (2001) calibration we obtain for this galaxy $\overline{M}_K = -5.60 \pm 0.08$. NGC 720 $\overline{M}_K$ is inconsistent with both the Jensen et al. mean value and the Liu et al. calibration at the three sigma level.

6. Summary and discussion

We find higher than standard K–band absolute amplitudes for NGC 1427 and NGC 720, with respect to the Jensen et al. (1998) mean value.

Other ellipticals appear to have larger than expected K–band SBF, including NGC 4489 and NGC 4365 in the Virgo cluster (Pahre & Mould 1994; Jensen et al. 1996; Jensen et al. 1998; Mei et al. 2001b), and NGC 1419 in the Fornax cluster (Liu et al. 2001). The $\overline{M}_K$ measured for these galaxies is about 0.5 mag brighter than the average. In combination with our new measurements, these results emphasize that K–band SBF are not as uniform as they would appear from the pioneering work of Jensen et al. (1998).

The Jensen et al. (1998) sample included around twenty bright red galaxies, and was the first sample large and precise enough to provide a first K–band SBF calibration. However, a larger K–band SBF sample spanning a larger range in colors and galaxy luminosity, as well as stellar population ages is necessary to derive a correct calibration and use this band in distance measurements.

A first step in this direction was made by Liu et al. (2001), whose measurements cover a $V-I$ range from 1.05 to 1.25 mag. If we compare our results with the Liu et al. (2001) calibration, our measurement for NGC 1427, using the I–band SBF Fornax distance modulus, is marginally consistent with the predicted $\overline{M}_K$. However, from the individual I–band SBF distance modulus we obtain a higher $\overline{M}_K$ than their calibration at the three sigma level. The high $\overline{M}_K$ for NGC 720 is not consistent with either the Jensen et al. mean value or the Liu et al. calibration at the three sigma level.

Recent stellar population models (Jensen et al. 1998; Liu et al. 2000; Blakeslee et al. 2001; Mei et al. 2001b) suggest that K–band SBF are more affected by age and metallicity changes than I–band SBF. From

Table 4. Absolute K–band surface brightness as a function of distance derived for NGC 1427 and NGC 720 using various distance indicators. For NGC 1427, member of the Fornax cluster, we also indicate the distances derived for the cluster.

	NGC 1427		NGC 1427 (Fornax)		NGC 720		comment
method	$(m-M)$	M_K(SBF)	$(m-M)$	M_K(SBF)	$(m-M)$	M_K(SBF)	
GCLF	31.02 ± 0.25	-5.71 ± 0.26	31.35 ± 0.16	-6.04 ± 0.18	31.67 ± 0.29	-5.89 ± 0.29	
GCLF			31.38 ± 0.15	-6.07 ± 0.17			Ferrarese et al. (2000a) in V
GCLF			31.76 ± 0.31	-6.45 ± 0.32			Ferrarese et al. (2000a) in B
I–SBF	31.86 ± 0.26	-6.55 ± 0.27	31.49 ± 0.04	-6.18 ± 0.09	32.21 ± 0.17	-6.43 ± 0.18	Tonry et al. (2001)
rec. vel.	31.47 ± 0.23	-6.16 ± 0.24			31.89 ± 0.22	-6.11 ± 0.23	$H_0 = 72 \pm 8$ km s^{-1} Mpc^{-1}
divers			31.52 ± 0.03	-6.21 ± 0.09			Ferrarese et al. (2000a) in B
Cepheids			31.60 ± 0.04	-6.29 ± 0.09			Ferrarese et al. (2000a)
mean		$-6.14, \sigma = 0.27$		$-6.20, \sigma = 0.18$		$-6.14, \sigma = 0.24$	

Bruzual & Charlot (2001) models, Liu et al. (2000, 2001) and Mei et al. (2001b) predict that the presence of young populations and high metallicities will increase the amplitude of the fluctuations, while low metallicities will lower their value. Stellar populations that dominate the K–band SBF are mostly those with metallicity close to solar and an age range from roughly 12 to 18 Gyr, but including some populations as young as ≈2 Gyr. The Blakeslee et al. (2001) models predict a comparable spread in age and a much wider spread in metallicity. They also predict higher amplitude fluctuations in younger populations, but a much weaker metallicity dependence.

The studies above mostly focused on single-burst, single-population galaxy simulations. Liu et al. (2001) (see also Mei et al. 2001b) demonstrate how brighter K–band SBF can be produced by a second burst which produces a younger population mixed with an old population. Such a model might apply to NGC 720. In fact, optical spectra of this galaxy suggest the presence of such a younger population (Trager et al. 2001).

However, there is no evidence for a young populations in NGC 1427 from line indices (Trager et al. 2000; Kuntschner 2000) and its metallicity is not unusual either. Thus, we do not expect high K–band SBF due to stellar population anomalies from present data. NGC 1427 remains puzzling. In this galaxy, the K–band SBF might trace stellar population features that do not influence the broad band colors nor the typical line indices.

In summary, our measurements underline once more the need for a better understanding of K–band SBF before using this technique as a reliable distance indicator to individual galaxies. Deviations from the canonical calibration value of $\overline{M}_K$ could be a complementary indicator of interesting stellar population anomalies that might not be detected with broad band or line indices observations.

References

Ajhar, E. A., Lauer, T. R., Tonry, J. L., et al. 1997, AJ, 114, 626

Ashman, K. M., Conti, A., & Zepf, S. E. 1995, 110, 1164

Bertin, E., & Arnouts, S. 1996, A&AS, 117, 393

Blakeslee, J. P., & Tonry, J. L. 1995, ApJ, 442, 579

Blakeslee, J. P., Ajhar, E. A., & Tonry, J. L. 1999a, in Post-Hipparcos Cosmic Candles, ed. A. Heck, & F. Caputo (Boston: Kluwer), 181

Blakeslee, J. P., Davis, M., Tonry, J. L., et al. 1999b, ApJ, 527, L73

Blakeslee, J. P., Vazdekis, A., & Ajhar, E. A. 2001, MNRAS, 320, 193

Bruzual, A. G., & Charlot, S. 2001, in preparation

Cowie, L. L., Gardner, J. P., Hu, E. M., et al. 1994, ApJ, 434, 114

Della Valle, M., Kissler-Patig, M., Danziger, J., & Storm, J. 1998, MNRAS, 299, 267

de Vaucouleurs, G., de Vaucouleurs, A., Corwin, J. R., et al. 1991, Third Reference Catalogue of Bright Galaxies (New York: Springer Verlag)

de Vaucouleurs, G. 1993, ApJ, 415, 10

Drenkhahn, G., & Richtler, T. 1999, A&A, 349, 877

Drinkwater, M. J., Gregg, M. D., & Colless, M. 2001, ApJ, 548, L142

Ferrarese, L., Mould, J. L., Kennicutt, R. C. et al. 2000a, ApJ, 529, 745

Ferrarese, L., Ford, H. C., Huchra, J., et al. 2000b, ApJS, 128, 431

Gebhardt, K., & Kissler-Patig, M. 2000, AJ, 118, 1526

Grillmair, C. J., Forbes, Duncan A., Brodie, Jean P. et al. 1999, AJ, 117, 167

Hunt, L. K., Mannucci, F., Testi, L., et al. 1998, AJ, 115, 2594

Jensen, J. B., Luppino, G. A., & Tonry, J. L. 1996, ApJ, 468, 519

Jensen, J. B., Tonry, J. L., & Luppino, G. A. 1998, ApJ, 505, 111

Jensen, J. B., Tonry, J. L., & Luppino, G. A. 1999, ApJ, 510, 71

Jensen, J. B., Tonry, J. L., Thomson, R. I. et al. 2001, ApJ, 550, 503

Kissler-Patig, M. 2000, Rev. Mod. Astron. 13, ed. R. Schielicke, 13

Kissler-Patig, M., Richtler, T., & Hilker, M. 1996, A&A, 308, 704

Kissler-Patig, M., Kohle, S., Hilker, M., et al. 1997, A&A, 319, 470

Kohle, S., Kissler-Patig, M., Hilker, M., et al. 1996, A&A, 309, 39

Kuntschner, H. 2000, MNRAS, 315, 184
Lauer, T. R., & Postman, M. 1992, ApJ, 400, L47
Lauer, T. R., & Postman, M. 1994, ApJ, 425, 418
Lauer, T. R., Tonry, J. L., Postman, M., et al. 1998, ApJ, 499, 577
Liu, M., Charlot, S., & Graham, J. R. 2000, ApJ, 543, 644
Liu, M., Graham, J. R., & Charlot, S. 2001, submitted to ApJ (private communication)
Luppino, G. A., & Tonry, J. L. 1993, ApJ, 410, 81
Madore, B. F., Freedman, W. L., & Silbermann, N. 1999, ApJ, 515, 29
McMillan, R., Ciardullo, R., & Jacoby, G. H. 1993, ApJ, 416, 62
Mei, S., Silva, D. R., & Quinn, P. J. 1999, ASP Conf. Ser. 167, ed. D. Egret, & A. Heck., 279
Mei, S., Silva, D. R., & Quinn, P.J. 2000, A&A, 361, 68
Mei, S., Silva, D. R., & Quinn, P. J. 2001a, A&A, 366, 54
Mei, S., Quinn, P. J., & Silva, D. R. 2001b, A&A, 371, 779
Pahre, M. A., & Mould, J. R. 1994, ApJ, 433, 567
Pahre, M. A., Mould, J. R., Dressler, A., et al. 1999, ApJ, 515, 79
Poulain, P. 1988, A&AS, 72, 215
Poulain, P., & Nieto, J.-L. 1994, A&AS, 103, 573
Press, W. H., Flannery, B. P., Teukolsky, S. A., et al. 1992, Numerical Recipes (Cambridge University Press, New York)
Schlegel, D. J., Finkbeiner, D. P., & Davis, M. 1998, ApJ, 500, 525
Sodemann, M., & Thomsen, B. 1995, AJ, 110, 179
Sodemann, M., & Thomsen, B. 1996, AJ, 111, 208
Thomsen, B., Baum, William, A., Hammergren, M., et al. 1997, ApJ, 483, L37
Tonry, J. L., & Schneider, D. P. 1988, AJ, 96, 807
Tonry, J. L., Ajhar, E. A., & Luppino, G. A. 1990, AJ, 100, 1416
Tonry, J. L., Blakeslee, J. P., Ajhar, E. A., et al. 1997, ApJ, 475, 399
Tonry, J. L., Blakeslee, J. P., Ajhar, E. A., et al. 2000, ApJ, 530, 625
Tonry, J. L., Dressler, A., Blakeslee, J. P., et al. 2001, ApJ, 546, 681
Trager, S. C., Faber, S. M., Worthey, G., et al. 2000, AJ, 120, 165
Tully, R. B. 1988, Nearby Galaxies Catalog (Cambridge University Press)
Wainscoat, R., & Cowie, L. 1992, AJ, 101, 332